

## EVN and MERLIN observations of an OH maser ring and a starburst continuum in III Zw 35

Ylva M. Pihlström, John E. Conway, and Roy S. Booth

*Onsala Space Observatory, S-439 92 Onsala, Sweden*

**Abstract.** We report on high-sensitivity EVN and MERLIN observations of the OH maser emission and continuum in the luminous infrared galaxy III Zw 35. Earlier VLBI observations have shown two compact maser clumps containing 40%–50% of the single-dish flux. In addition to these compact masers, we detect more diffuse maser emission which lies in a clear ring structure of radius  $r \sim 22$  pc. The ring appears inclined to the line of sight and the compact masers occur at the tangent points. This structure suggests that the compact and diffuse masers appear different because of geometrical effects and not pumping or other physical conditions. Our observations reveal a velocity gradient along the western side of the disc which indicates rotation. The 18 cm continuum radiation is resolved into a few unresolved sources, plus more diffuse emission and is broadly consistent with emission originating in a starburst.

### 1. Introduction

III Zw 35 is a typical OH megamaser galaxy; the host galaxy is one of the luminous infrared galaxies (LIRG) with an infrared luminosity of  $L_{FIR} \sim 3 \times 10^{11} L_{\odot}$ . It has two optical nuclei indicating a merging system, however, the radio emission and OH megamasers are only related to one of these nuclei. After the initial single-dish detection (Staveley-Smith et al. 1987), Montgomery & Cohen (1992) used MERLIN to investigate the OH megamaser emission in III Zw 35. They found that the maser emission was distributed more or less along a line, and that there was a velocity gradient along this line. However, later on Trotter et al. (1997) and Diamond et al. (1998) performed VLBA and global VLBI observations, which did not reveal this continuous distribution of maser emission. Instead these two high-resolution experiments found two compact clumps, one to the North and one to the South. Although there still was a velocity shift between these clumps, no emission was detected in between. It was argued that the MERLIN disc result was just due to blending between the two clumps. On the other hand, in the VLBI observations 40%–50% of the single dish flux was resolved out. Therefore, in our new observations the main aim was to find and to map this missing flux by using the intermediate range of baselines that is provided by the European VLBI Network (EVN) and MERLIN.

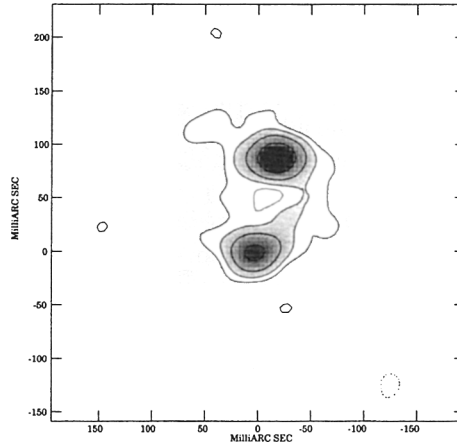


Figure 1. Contour map of the integrated 1667 MHz maser emission in III Zw 35 for the EVN and MERLIN combined array. At a distance of 110 Mpc 1 mas corresponds to 0.5 pc. The data has been averaged in frequency over all spectral channels showing OH maser emission. The data has been tapered by a Gaussian of value 0.3 at  $5M\lambda$  and the beam size is  $33.0 \times 28.7$  mas. Plotted contours are -1, 1, 2, 4 and 8 times the  $3\sigma$  rms noise of 2.7 mJy/beam.

## 2. The OH maser emission

Figure 1 plots the distribution of the total 1667 MHz OH maser emission observed with the combined EVN and MERLIN array. The two strongest components correspond to the two clumps of maser emission that were found in the VLBI observations. In addition we also detect more diffuse maser emission in two arcs between the compact components, and Fig. 1 also shows a region in the centre which is devoid of maser emission. Thus, it appears that the maser emission is distributed in a ring, and assuming circular orbits the plane of this ring is inclined with  $30^\circ$  to the line of sight. A velocity plot (not shown) reveals a velocity gradient from North to South. If we assume Keplerian rotation between these two compact components we find that the enclosed mass within a radius of 22 pc would be of the order of  $10^7 M_\odot$ .

Given the distribution of the compact and the diffuse maser emission, the simplest explanation to the OH maser emission is that it lies in a thick rotating ring. The velocity field implies ordered motion, which is consistent with such a geometry. Given that the masers occur in a ring structure, the difference between the compact and the diffuse maser emission is probably not due to any physical differences (like pumping rate or density etc.), but can be understood due to geometrical effects. The compact clumps then lie at positions of the ring where we have long path length. In order to generate strong maser emission we would expect the disc to be thick since we have an angle of  $30^\circ$  between the line of sight and the plane of the disc. Consistent with our ring model are our results from the 1665 MHz transition. We find weak 1665 MHz maser emission at the

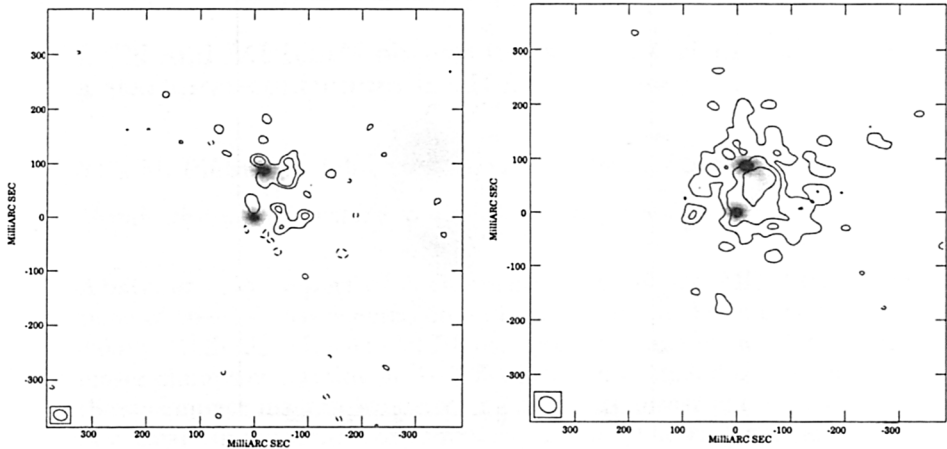


Figure 2. These maps display the continuum in contours and the 1667 MHz maser emission superposed in grey-scale. *a)* EVN + MERLIN combined continuum at a resolution of  $34 \times 28$  mas, plotted contours are -1, 1, 2 and 4 times the  $3\sigma$  rms noise of 0.27 mJy/beam. *b)* EVN-only naturally weighted map, resolution  $25.4 \times 19.2$  mas. Plotted contours are -3, 3, 6 and 12 times the  $1\sigma$  rms noise of 0.1 mJy/beam.

positions of the Northern and the Southern clump respectively, with velocities agreeing with that of the 1667 MHz emission. Estimating the ratio between the 1667 and 1665 MHz flux densities for the compact and diffuse masers respectively we find that these ratios are similar ( $\sim 8$ ), which implies that the pumping rate and the population inversion of the molecular energy levels are the same for the compact and diffuse masers.

### 3. The 18cm continuum results

Figure 2 plots the 18cm continuum detected in our observations. In Fig. 2a we plot the EVN+MERLIN map, with the continuum in contours and the 1667 MHz maser emission in greyscale. The main part of the emitted flux, around 35 mJy, is found in this diffuse extended continuum component which has a size of around 200 pc. Fig. 2b shows the EVN-only map at natural weighting, and here the continuum resolves into compact clumps of emission. This resembles what has been observed in a couple of other OH megamaser galaxies, like in Arp220 (Smith et al. 1998) and Mrk273 (Carilli & Taylor 1999). Different optical spectroscopical investigations have classified III Zw 35 both as a LINER and as a starburst. Therefore (as is the case for many LIRGs) it has not been clear what the dominant heating source is. However, the continuum we detect have no compact AGN component but instead a clumpy distribution which suggests that the energetically dominant source in this object is a starburst. Other arguments

for a starburst come for instance from the red IR colour of III Zw 35 which is more consistent with dust that is heated by a starburst rather than an AGN. Moreover, III Zw 35 lies on the radio-infrared correlation for starbursts, where the infrared radiation is thought to derive from a massive starburst, and the radio emission from supernova remnants which emit synchrotron radiation. In addition, CO observations imply a high starformation efficiency (Sanders et al. 1991).

Using the IR flux we can calculate the star formation rate to  $34 M_{\odot} \text{ yr}^{-1}$ , corresponding to a supernova rate of around  $1 \text{ yr}^{-1}$ . The total emitted non-thermal flux from the supernova remnants can then be estimated assuming a Galactic relation between the luminosity and the supernova rate. We find that the supernova remnants in III Zw 35 could account for  $\sim 9 \times 10^{22} \text{ W Hz}^{-1}$ , which is approximately what we detect in the diffuse component ( $\sim 6 \times 10^{22} \text{ W Hz}^{-1}$ ). Hence, a starburst could readily explain the diffuse emission we observe.

For the compact components there are at least two possibilities; the first one is that they are a population of very luminous young supernovae as has been suggested for the compact objects found in Arp220 (Smith et al. 1998). These objects would then have luminosities of a few times  $10^{21} \text{ W Hz}^{-1}$ , similar to the luminosity of one of the strongest radio supernovae observed (SN1986J; Weiler et al. 1990). We estimate that such luminous supernovae would have flux densities above our detection level for around 7 years, which is consistent with the number of clumps that we observe. However, in this scenario each supernova would have to be of the very luminous type. Another possibility is that the clumps of emission are instead nested supernova remnants. Indeed, there is support for clumpy starbursts, for example HST UV images of starforming galaxies reveal clusters and superstarclusters of sizes of a few to 10 pc (Meurer et al. 1995), close to the sizes of our compact clumps. Moreover, Smith et al. (1998) have made models of star formation in a sample of ULIRGs to see how well it fits the radio continuum emission that is observed. They found that a clumpy distribution of stars fits the data much better than a uniform starburst.

## References

- Carilli, C.L., & Taylor, G.B. 2000, *ApJ*, 533, L13  
Diamond, P.J., Lonsdale, C.J., Lonsdale, C.J., & Smith, H.E., 1999, *ApJ*, 511, 178  
Meurer, G.R., Heckman, T.M., Leitherer, C., Kinney, A., Robert, C., & Garnett, D.R. 1995, *AJ*, 110, 2665  
Montgomery, A.S., & Cohen, R.J. 1992, *MNRAS*, 254, 23  
Sanders, D.B., Scoville, N.Z., & Soifer, B.T. 1991, *ApJ*, 370, 158  
Smith, H.E., Lonsdale, C.J., & Lonsdale, C.J. 1998, *ApJ*, 492, 137  
Staveley-Smith, L., Cohen, R.J., Chapman, J.M., Pointon, L., & Unger, S.W. 1987, *MNRAS*, 226, 689  
Trotter, A.S., Moran, J.M., Greenhill, L.J., Zheng, X., & Gwinn, C.R. 1997, *ApJ*, 485, L79  
Weiler, K.W., Panagia, N., & Sramek, R. 1990, *ApJ*, 364, 611